



## High-order harmonic generation of the cyclo[18]carbon molecule irradiated by circularly polarized laser pulse

Shu-Shan Zhou(周书山), Yu-Jun Yang(杨玉军), Yang Yang(杨扬), Ming-Yue Suo(索明月), Dong-Yuan Li(李东垣), Yue Qiao(乔月), Hai-Ying Yuan(袁海颖), Wen-Di Lan(蓝文迪), and Mu-Hong Hu(胡木宏)

**Citation:** Chin. Phys. B, 2023, 32 (1): 013201. DOI: 10.1088/1674-1056/aca3a1

Journal homepage: <http://cpb.iphy.ac.cn>; <http://iopscience.iop.org/cpb>

**What follows is a list of articles you may be interested in**

---

### Multiple collisions in crystal high-order harmonic generation

Dong Tang(唐栋) and Xue-Bin Bian(卞学滨)

Chin. Phys. B, 2022, 31 (12): 123202. DOI: 10.1088/1674-1056/ac6b2c

### Probing subcycle spectral structures and dynamics of high-order harmonic generation in crystals

Long Lin(林龙), Tong-Gang Jia(贾铜钢), Zhi-Bin Wang(王志斌), and Peng-Cheng Li(李鹏程)

Chin. Phys. B, 2022, 31 (9): 093202. DOI: 10.1088/1674-1056/ac6943

### Generation of elliptical isolated attosecond pulse from oriented H<sub>2</sub><sup>+</sup> in a linearly polarized laser field

Yun-He Xing(邢云鹤), Jun Zhang(张军), Xiao-Xin Huo(霍晓鑫), Qing-Yun Xu(徐清芸), and Xue-Shen Liu(刘学深)

Chin. Phys. B, 2022, 31 (4): 043203. DOI: 10.1088/1674-1056/ac398b

### Generation of non-integer high-order harmonics and significant enhancement of harmonic intensity

Chang-Long Xia(夏昌龙), Yue-Yue Lan(兰悦跃), and Xiang-Yang Miao(苗向阳)

Chin. Phys. B, 2021, 30 (4): 043202. DOI: 10.1088/1674-1056/abd389

### Multiphoton quantum dynamics of many-electron atomic and molecular systems in intense laser fields

Peng-Cheng Li(李鹏程), Shih-I Chu

Chin. Phys. B, 2020, 29 (8): 083202. DOI: 10.1088/1674-1056/ab9c0f

---

# High-order harmonic generation of the cyclo[18]carbon molecule irradiated by circularly polarized laser pulse

Shu-Shan Zhou(周书山)<sup>1</sup>, Yu-Jun Yang(杨玉军)<sup>2</sup>, Yang Yang(杨扬)<sup>1</sup>, Ming-Yue Suo(索明月)<sup>1</sup>, Dong-Yuan Li(李东垣)<sup>1</sup>, Yue Qiao(乔月)<sup>2</sup>, Hai-Ying Yuan(袁海颖)<sup>2</sup>, Wen-Di Lan(蓝文迪)<sup>2</sup>, and Mu-Hong Hu(胡木宏)<sup>1,†</sup>

<sup>1</sup>*School of Physics and Electronic Technology, Liaoning Normal University, Dalian 116029, China*

<sup>2</sup>*Institute of Atomic and Molecular Physics, Jilin University, Changchun 130012, China*

(Received 22 September 2022; revised manuscript received 11 November 2022; accepted manuscript online 17 November 2022)

High-order harmonic generation of the cyclo[18]carbon ( $C_{18}$ ) molecule under few-cycle circularly polarized laser pulse is studied by time-dependent density functional theory. Compared with the harmonic emission of the ring molecule  $C_6H_6$  having similar ionization potential, the  $C_{18}$  molecule has higher efficiency and cutoff energy than  $C_6H_6$  with the same laser field parameters. Further researches indicate that the harmonic efficiency and cutoff energy of the  $C_{18}$  molecule increase gradually with the increase of the laser intensity of the driving laser or decrease of the wavelength, both are larger than those of the  $C_6H_6$  molecule. Through the analysis of the time-dependent evolution of the electronic wave packets, it is also found that the higher efficiency of harmonic generation can be attributed to the larger spatial scale of the  $C_{18}$  molecule, which leads to a greater chance for the ionized electrons from one atom to recombine with others of the parent molecule. Selecting the suitable driving laser pulse, it is demonstrated that high-order harmonic generation in the  $C_{18}$  molecule has a wide range of applications in producing circularly polarized isolated attosecond pulse.

**Keywords:** time-dependent density functional theory, high-order harmonic generation, circularly polarized attosecond pulse

**PACS:** 32.80.Rm, 42.50.Hz, 42.65.Ky

**DOI:** 10.1088/1674-1056/aca3a1

## 1. Introduction

The interaction of atoms, molecules, or crystals with intense laser pulse can induce a variety of strong-field physical phenomena, such as tunneling ionization,<sup>[1]</sup> above-threshold ionization,<sup>[2]</sup> non-sequential double ionization,<sup>[3,4]</sup> and high-order harmonic generation (HHG).<sup>[5–9]</sup> Among them, HHG tends to be an important resource for the production of attosecond pulses<sup>[10]</sup> because of its ability of amplifying the frequency of the incident laser by hundreds of times. With the in-depth developments of harmonic research, it has been found that elliptically or circularly polarized HHG and ultrashort pulses can be generated by controlling the polarization of harmonic emission, which have important applications in x-ray magnetic circular dichroism,<sup>[11]</sup> ultrafast spin dynamics,<sup>[12]</sup> chirality recognition,<sup>[13]</sup> etc. Therefore, the research on circularly polarized HHG and ultrashort pulses has become one of the hotspots in the field of strong-field physics.

The HHG mechanism can usually be described with the “three-step” model theory.<sup>[14]</sup> Firstly, valence electrons are tunnel ionized by the incident laser field, then the ionized electrons are accelerated by the laser electric field, and finally, some of these ionized electrons have opportunities to recombine with the parent ion and return to the ground state after they release the kinetic energy by emitting HHG. With this mechanism, more strong and high-frequency harmonic emission of atomic gas has been generated by linearly polarized

laser pulse (LPLP). However, for atomic gas driven by circularly polarized laser pulse (CPLP), the probability of recombination between the ionized electrons and the nucleus is very small since the main movement area of the ionized electrons is far away from the nucleus, then it is not easy to observe the circularly polarized harmonic emission. In order to solve this problem, a scheme to generate circularly polarized HHG effectively and directly is designed, a circularly polarized fundamental field with frequency  $\omega$  and its counterrotating second harmonic  $2\omega$  are used to irradiate atomic or molecular gas targets simultaneously to generate the circularly polarized harmonics.<sup>[15]</sup> The atomic gas driven by the counter-rotating bicircular field can emit left-handed and right-handed harmonics alternately, and the intensity of the circularly polarized harmonics is close to that of linearly polarized harmonics.<sup>[16–19]</sup> But the helicities of different harmonic orders generated in a spectrum range are different, and the spectral width is not wide enough to synthesize ultrashort pulse, which cannot meet the requirement of ultrafast measurements. Some methods have been attempted to obtain the harmonic spectra with wide range and single helicity. In 2006, a series of circularly polarized harmonics were obtained at the end of the harmonic plateau using the combination of the circularly polarized laser field and the electrostatic field.<sup>[20]</sup> From 2012 to 2013, the circularly polarized isolated attosecond pulses (IAP) were obtained by combining the circularly polarized laser field and linearly polarized laser field, or combining the elliptically polarized

<sup>†</sup>Corresponding author. E-mail: humuhong@163.com

laser field and terahertz laser field.<sup>[21,22]</sup> Two years later, the circularly polarized IAPs were synthesized using the circularly polarized supercontinuum spectrum obtained with the spatially inhomogeneous field method,<sup>[23]</sup> the elliptically polarized IAP was generated by adjusting the time delay between the two circularly polarized laser fields.<sup>[24]</sup> In 2017, some studies focusing on the efficiency were carried out, the circularly polarized attosecond pulses were obtained efficiently by adjusting the relative frequency ratio of the bichromatic circularly polarized driving laser field,<sup>[25]</sup> the emission efficiency of left-handed or right-handed harmonics was selectively improved by adjusting the relative intensity ratio of the bichromatic circularly polarized driving laser field.<sup>[26]</sup> In 2018, the scheme to produce high ellipticity IAP with tri-circularly fields was proposed in the study of optical chirality.<sup>[27]</sup> In 2019, nearly circular attosecond pulse trains were obtained with a proper ellipticity  $\xi$  for  $\omega$ – $3\omega$  driving laser field, which consists of a circularly polarized field with its coplanar counter-rotating elliptical harmonic pulse.<sup>[28]</sup> In 2020, the counter-rotating bicircular field containing a time delay and having an appropriate orbital angular momentum was selected as a driving laser field, the attosecond pulse train was generated.<sup>[29]</sup> Based on the accuracy controls of the driving laser field, the methods mentioned above have made considerable progresses to meet the increasing demands, however, the higher requirements of performing actual operations in experiments are still unsatisfied.

As the gas target is not an atom but a molecule or a solid, the harmonics irradiated by the interaction with the CPLP exhibit abundant characteristics due to the high electron density and multicenter structure.<sup>[30–33]</sup> The efficiency of harmonic emission produced by a circularly polarized laser field interacting with small linear molecules is higher than that of atoms with the same ionization potential and the same laser field,<sup>[34,35]</sup> aligned small molecules can produce low-order harmonic in a circularly polarized laser field.<sup>[36,37]</sup> A large amount of theoretical and experimental results have been obtained in the past decades.<sup>[38–41]</sup> As an important molecule target, the harmonic emission of  $C_6H_6$  molecule in a circularly polarized laser field has been studied. With the weak laser intensity, there is only one plateau in the harmonic spectrum, the allowed harmonic orders are  $6k \pm 1$  ( $k = 1, 2, \dots$ ) due to the re-collision mechanism. While with the higher laser intensity, there are multiple plateaus in the harmonic spectrum because of the transitions from bound state to bound state.<sup>[42–44]</sup> Using the interaction of ring molecule  $C_6H_6$  with CPLP, the 108 as circularly polarized IAP has been obtained theoretically.<sup>[45]</sup> The fact that  $C_6H_6$  molecule can emit HHG in a circularly polarized laser field is inspiring, but its harmonic energy is really low and intensity is weak.

The cyclo[18]carbon ( $C_{18}$ ), a synthesized alkynes con-

taining 18 sp-hybridized carbon atoms, was prepared and directly observed by Kaiser *et al.* in 2019.<sup>[46]</sup> As a potential molecule target, cyclo[18]carbon has been theoretically investigated, because of its unique ring structure and dual 18-center  $\pi$  delocalization feature. Compared with the  $C_6H_6$  molecule, the  $C_{18}$  molecule has unusual characteristics and properties, the ability of having strong harmonic emission in circularly polarized laser field makes it possible to be a powerful candidate used to generate the high-intensity isolated attosecond pulse. Therefore, it is necessary to apply a reliable theoretical method to accomplish a thorough research on the harmonic emission of the  $C_{18}$  molecule.

In this work, the time-dependent density functional theory (TDDFT)<sup>[47]</sup> is employed to study the HHG of the  $C_{18}$  molecule with larger spatial scale in circularly polarized laser field. The harmonic spectra obtained from the interaction of  $C_{18}$  molecule with CPLP are analyzed and compared with those of  $C_6H_6$  molecule, the effects of the intensity and wavelength of the incident circularly polarized driving laser field on the harmonic emission are discussed. And the scheme to obtain two attosecond pulses with opposite polarizations is explained in detail, which is hoped to be useful to generate the isolated attosecond pulse efficiently and reliably.

## 2. Theory and models

The TDDFT method is widely used to study the HHG of molecules driven by intense laser fields,<sup>[48–51]</sup> the HHG of the  $C_6H_6$  molecule<sup>[52]</sup> and more complex solid-state systems<sup>[40,53]</sup> calculated by TDDFT are also in good agreement with the experimental measurements.

For a many-body system evolving from a given initial state, a one-to-one mapping between the time-dependent external potential and the time-dependent single-electron density is established with Runge–Gross theorem.<sup>[47]</sup> In the length gauge and dipole approximation, the electrons of molecular systems driven by circularly polarized laser pulse follow the equations of time-dependent Kohn–Sham (KS) orbitals  $\psi_i(\mathbf{r}, t)$ , which is given (atomic units are used hereinafter) by

$$i \frac{\partial}{\partial t} \psi_i(\mathbf{r}, t) = \left[ -\frac{1}{2} \nabla^2 + V_{KS}[\rho](\mathbf{r}, t) \right] \psi_i(\mathbf{r}, t), \quad i = 1, \dots, N, \quad (1)$$

where  $i$  is the orbital index,  $N$  is the number of Kohn–Sham orbitals,  $\rho(\mathbf{r}, t)$  is the time-dependent electron density,  $\rho(\mathbf{r}, t) = 2 \sum_{j=1}^N |\psi_j(\mathbf{r}, t)|^2$ .

The Kohn–Sham potential  $V_{KS}[\rho](\mathbf{r}, t)$ , a function of  $\rho(\mathbf{r}, t)$ , is defined as

$$V_{KS}[\rho](\mathbf{r}, t) = V_{xc}[\rho](\mathbf{r}, t) + V_H[\rho](\mathbf{r}, t) + V_{ne}(\mathbf{r}) + V_{laser}(\mathbf{r}, t), \quad (2)$$

where the first term  $V_{xc}[\rho](\mathbf{r}, t)$  is the exchange–correlation potential describing the nonperturbative many-body effect, which is represented with general gradient approximation (GGA) in the Perdew–Burke–Ernzerhof (PBE) form.<sup>[54]</sup> The second term  $V_H[\rho](\mathbf{r}, t)$  is the Hartree potential, the third term  $V_{ne}(\mathbf{r})$  is the electron–ion interactions described with norm-conserving Troullier–Martins pseudopotentials<sup>[55]</sup> in the parametrization of Kleinman–Bylander,<sup>[56]</sup> and the last term  $V_{laser}(\mathbf{r}, t)$  is the external potential caused by the interaction between the external laser field and the molecule, it is given as  $V_{laser}(\mathbf{r}, t) = \mathbf{r} \cdot \mathbf{E}(t)$ , where  $\mathbf{E}(t)$  is the circularly polarized laser field,

$$\mathbf{E}(t) = \frac{E_0}{\sqrt{2}} f(t) \cos(\omega_0 t) \hat{e}_x + \frac{E_0}{\sqrt{2}} f(t) \sin(\omega_0 t) \hat{e}_z, \quad (3)$$

and the envelope of the laser field is a Gaussian envelope,  $f(t) = e^{-4 \ln 2 \left( \frac{t-t_0}{\tau} \right)^2}$ .

The time-dependent Kohn–Sham orbital wavefunctions are propagating on a real-space grid with real-time. The time propagating method can be characterized by the time-reversal symmetry. Here we use the approximated enforced time-reversal symmetry (AETRS),<sup>[57]</sup> the time step is 0.00192 fs.

In order to avoid the unphysical effects caused by the reflection of the electron wave packet from the boundary, we multiply a complex absorption potential (CAP)<sup>[58]</sup>

$$V_{\text{absorb}}(r) = \begin{cases} 0, & 0 < r < r_{\text{max}}, \\ i\eta \sin^2 \left[ \frac{(r - r_{\text{max}})\pi}{2L} \right], & r_{\text{max}} < r < r_{\text{max}} + L, \end{cases} \quad (4)$$

where  $L = 10$  a.u. and  $\eta = -0.8$  a.u. are the width and height of the absorbing potential, respectively.

The corresponding harmonic spectrum can be obtained from the time-dependent dipole acceleration  $\mathbf{a}(t)$  as<sup>[59]</sup>

$$H(\omega) = \left| \int \mathbf{a}(t) e^{-i\omega t} dt \right|^2, \quad (5)$$

where  $\mathbf{a}(t) = -\int \rho(\mathbf{r}, t) \nabla H_{\text{KS}} d^3\mathbf{r}$ ,  $H_{\text{KS}} = -(1/2)\nabla^2 + V_{\text{KS}}[\rho](\mathbf{r}, t)$ . The components of the  $\mathbf{a}(t)$  in  $x$  and  $z$  directions are defined as

$$\mathbf{a}_p(t) = -\int d^3\mathbf{r} \rho(\mathbf{r}, t) \nabla \{V_H[\rho](\mathbf{r}, t) + V_{ne}(\mathbf{r}) + V_{xc}[\rho](\mathbf{r}, t)\} - N \cdot \mathbf{E}_p(t), \quad p = x, z, \quad (6)$$

where  $x$  and  $z$  represent the laser polarization directions.

Through the Fourier transformation of  $\mathbf{a}_p(t)$ , we can get

$$\tilde{\mathbf{a}}_p(\omega) = \int \mathbf{a}_p(t) e^{-i\omega t} dt, \quad p = x, z. \quad (7)$$

Then the harmonic ellipticity<sup>[60]</sup> is obtained as

$$\varepsilon = \frac{|\tilde{\mathbf{a}}_+| - |\tilde{\mathbf{a}}_-|}{|\tilde{\mathbf{a}}_+| + |\tilde{\mathbf{a}}_-|}, \quad (8)$$

where  $\tilde{\mathbf{a}}_{\pm} = (1/\sqrt{2})(\tilde{\mathbf{a}}_x \pm i\tilde{\mathbf{a}}_z)$ .

Choosing the harmonic coherent superposition in a certain energy range, the attosecond pulse can be synthetized, its intensity is given as follows:

$$I(t) = \left| \int_q \tilde{\mathbf{a}}_q e^{iq\omega_0 t} \right|^2, \quad (9)$$

where  $q$  is the harmonic order.

### 3. Results and discussion

The ground state of the system is prepared with the static density functional theory (DFT), the KS orbitals  $\psi_i(\mathbf{r}, t)$  are solved numerically using the Octopus code.<sup>[61–63]</sup> The simulation box selected in the present work is designed with  $|r_x| \leq 70$  a.u.,  $|r_y| \leq 30$  a.u., and  $|r_z| \leq 70$  a.u., the spacing step is 0.4 a.u. For the  $\text{C}_{18}$  and  $\text{C}_6\text{H}_6$  molecules, their centers are at the coordinate origin, all the nucleus are fixed, and the molecule is located on the  $x$ – $z$  plane, which is coplanar with the polarization direction of the circularly polarized laser field. The structure (the knotted model) of  $\text{C}_{18}$  used in this work is shown in Fig. 1, and the C–C bond length is alternating between 1.22 Å and 1.34 Å, the bond angle is always 160°. For the  $\text{C}_6\text{H}_6$  molecule, the C–C bond length is 1.399 Å, and the C–H bond length is 1.486 Å. The molecular maximum nuclear distances (diameter) of the  $\text{C}_{18}$  and  $\text{C}_6\text{H}_6$  molecules are 7.380 Å and 4.962 Å, respectively. The calculated highest occupied molecular orbital (HOMO) energies of the  $\text{C}_{18}$  and  $\text{C}_6\text{H}_6$  molecules are 7.589 eV and 9.656 eV, respectively.

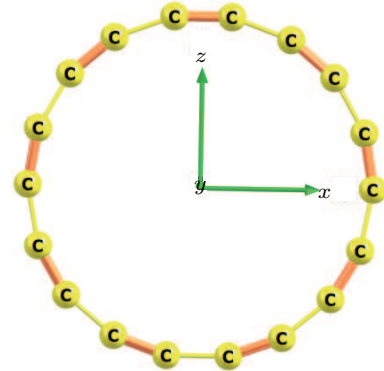
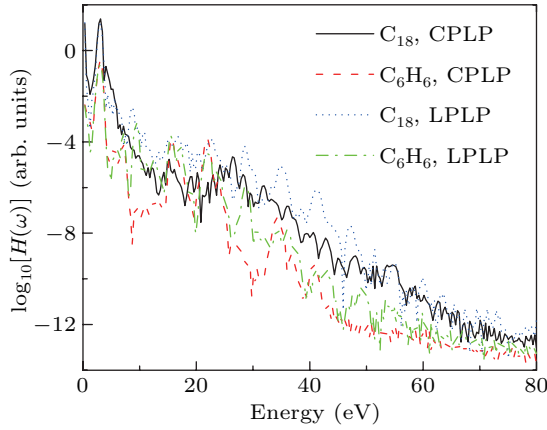


Fig. 1. The structure of cyclo[18]carbon ( $\text{C}_{18}$ ).<sup>[64]</sup>

The harmonic spectra of  $\text{C}_{18}$  molecule driven by CPLP and LPLP are plotted in Fig. 2, the harmonic spectra of  $\text{C}_6\text{H}_6$  molecule driven by CPLP and LPLP are also plotted to draw comparisons. The wavelength of the CPLP is 400 nm, the peak intensity is  $I = 1.12 \times 10^{14}$  W/cm<sup>2</sup>, and the full width at half maximum (FWHM) is  $\tau = 7.92$  fs. The parameters of LPLP are the same as those of CPLP. The black solid line and red dashed line in Fig. 2 represent the harmonic spectra of  $\text{C}_{18}$  and  $\text{C}_6\text{H}_6$  molecules in CPLP, respectively, and the blue dotted line and green dotted dashed line represent the harmonic spectra of  $\text{C}_{18}$  and  $\text{C}_6\text{H}_6$  molecules in LPLP, respectively.





**Fig. 2.** Harmonic spectra obtained from the interaction of  $C_{18}$  and  $C_6H_6$  molecules with CPLP.  $I = 1.12 \times 10^{14} \text{ W/cm}^2$ ,  $\lambda = 400 \text{ nm}$ ,  $\tau = 7.92 \text{ fs}$ .

For  $C_{18}$  and  $C_6H_6$  molecules, the intensities of harmonic spectra generated in different polarized laser fields approach to each other closely. All the intensities of harmonic spectra have obvious tendencies of cutoff, and the cutoff energy of harmonic spectrum driven by CPLP is smaller than that by LPLP. As shown in Fig. 2, both molecules have strong harmonic emission in CPLP, the harmonic efficiency of the  $C_{18}$  molecule is higher than that of the  $C_6H_6$  molecule, only several harmonics with higher efficiency appear in  $C_6H_6$  molecule, which locate at about 20 eV. In addition, the cutoff energy of the  $C_{18}$  molecule is larger than that of the  $C_6H_6$  molecule, and its range of harmonic spectra is more wider. According to the selection rules of harmonic emission for a molecule driven by CPLP, the harmonic emission of  $C_{18}$  molecule should follow the  $9m \pm 1$  ( $m = 0, 1, \dots$ ) selection rule due to its  $C_9$  symmetry. But the harmonic emission of the  $C_{18}$  molecule does not follow the selection rule as analyzed in  $C_6H_6$  molecule in our previous article.<sup>[44]</sup> Also shown in Fig. 2, there is no prominent peak in the integer order of the harmonic spectrum of  $C_{18}$  molecule, only some small peaks appear in the vicinity, it may indicate that there is symmetry breaking caused by the complexity of the  $C_{18}$  molecular structure.

To ascertain the reasons of this phenomenon, the time-dependent evolution of the ionized electron wave packet for  $C_{18}$  molecule driven by CPLP is studied, the results are shown in Fig. 3, the corresponding evolution process of  $C_6H_6$  molecule is also shown in the same figure. The red frames represent the main ranges of electron density distribution for the ground state of the molecules. It can be seen from Figs. 3(a) and 3(e), the electron density distribution range of  $C_{18}$  molecule is circular, which is clearly bigger than that of  $C_6H_6$  molecule. Figures 3(b)–3(d) and 3(f)–3(h) are the time-dependent evolutions of the ionized electron wave packet of  $C_{18}$  molecule and  $C_6H_6$  molecule, respectively. In order to monitor the evolutionary behavior clearly, the initial state has been subtracted from the wave packet.

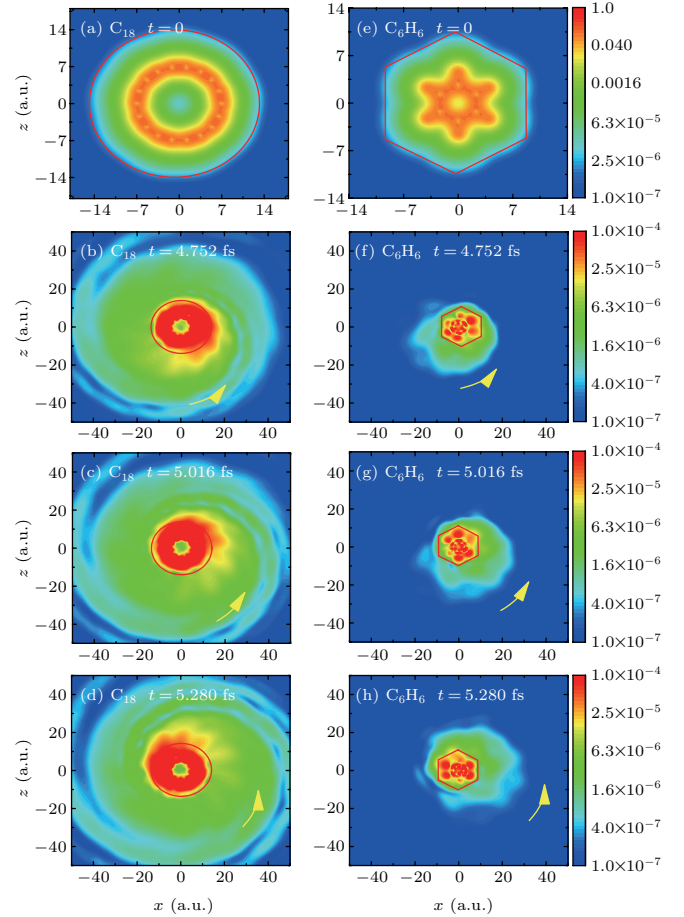


**Fig. 3.** Instantaneous electron density distribution in CPLP. The  $C_{18}$  molecule: (a)  $t = 0$ , (b)  $t = 4.752 \text{ fs}$ , (c)  $t = 5.016 \text{ fs}$ , (d)  $t = 5.280 \text{ fs}$ . The  $C_6H_6$  molecule: (e)  $t = 0$ , (f)  $t = 4.752 \text{ fs}$ , (g)  $t = 5.016 \text{ fs}$ , (h)  $t = 5.280 \text{ fs}$ .

Actually, the wave packet of ionized electrons driven by CPLP appears counterclockwise rotation. However, there is an obvious difference between the  $C_{18}$  molecule and  $C_6H_6$  molecule. For the former, the ionized electrons have opportunity to recombine with other atoms of the parent ion due to the large number of ionized electrons, then the intensity of high harmonics generated by CPLP is close to that by LPLP. For the latter, the ionized electrons driven by laser pulse move around the ion, the electron density of the initial state covers a wider range due to its large space size. Moreover, the characters of great number of atoms and the ring structure make the probability of recombination between the ionized electrons and other atoms tend to increase as they are driven by the laser electric field, which provide more chances for the recombination ion to fulfill the transitions leading to the higher harmonic intensity.

In order to study the HHG of the  $C_{18}$  molecule driven by CPLP profoundly, the effects of intensity and wavelength of CPLP on harmonic emission are investigated systematically. First, the harmonic spectra of  $C_{18}$  molecule is obtained by changing the intensity of the incident laser pulse. Based on the same laser pulse, the results obtained with different laser intensities are compared with those of  $C_6H_6$  molecule, all of them are shown in Fig. 4. It is found that there is little dif-

ference between the efficiencies of the two molecules at weak intensity. With the increasing of the laser intensity, the narrower difference between the harmonic emission efficiencies tends to enlarge, and  $C_{18}$  molecule is more efficient at higher laser intensity. It is also found the cutoff energies of both molecules have the same rules of variation along the increase of the laser intensity. Compared the cases of different laser intensities with fixed wavelength, it can be inferred that it is easier for  $C_{18}$  molecule to have higher efficiencies of harmonic emission driven by CPLP due to its larger ring structure.

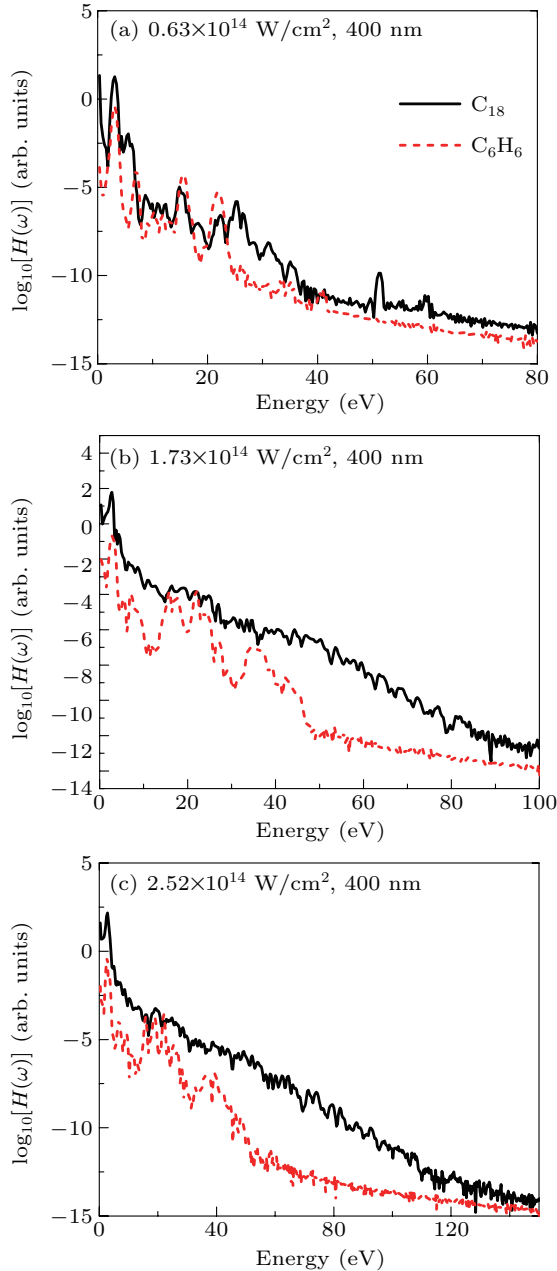


**Fig. 4.** The HHG spectra of  $C_{18}$  and  $C_6H_6$  molecules driven by CPLP with different laser intensities: (a)  $0.63 \times 10^{14} \text{ W/cm}^2$ , (b)  $1.75 \times 10^{14} \text{ W/cm}^2$ , and (c)  $2.52 \times 10^{14} \text{ W/cm}^2$ .

Then we change the wavelength of the incident CPLP to investigate the effect on harmonic emission. With the fixed intensity  $I = 1.12 \times 10^{14} \text{ W/cm}^2$ , the wavelengths are selected at 800 nm, 400 nm, and 200 nm, respectively. The har-

monic spectra are shown in Figs. 5(a)–5(c). As can be seen from Fig. 5, the harmonic cutoff energies of  $C_{18}$  molecule and  $C_6H_6$  molecule gradually become larger as the wavelength decreases, but the cutoff energy of  $C_{18}$  molecule is always larger than that of  $C_6H_6$  molecule. For 800 nm driving laser pulses, the harmonic emission efficiency of the  $C_{18}$  molecule is about 2 orders of magnitude higher than that of the  $C_6H_6$  molecule. For 400 nm and 200 nm driving laser pulses, the efficiency of several harmonic orders of the  $C_6H_6$  molecule is higher than those of the  $C_{18}$  molecule in the low energy region ( $< 30 \text{ eV}$ ), as for the high energy region ( $> 30 \text{ eV}$ ), the harmonic efficiency of the  $C_{18}$  molecule is higher than that of the  $C_6H_6$  molecule, it may imply that the higher harmonic emission efficiency of  $C_{18}$  molecule in high energy region is caused by its larger space size.

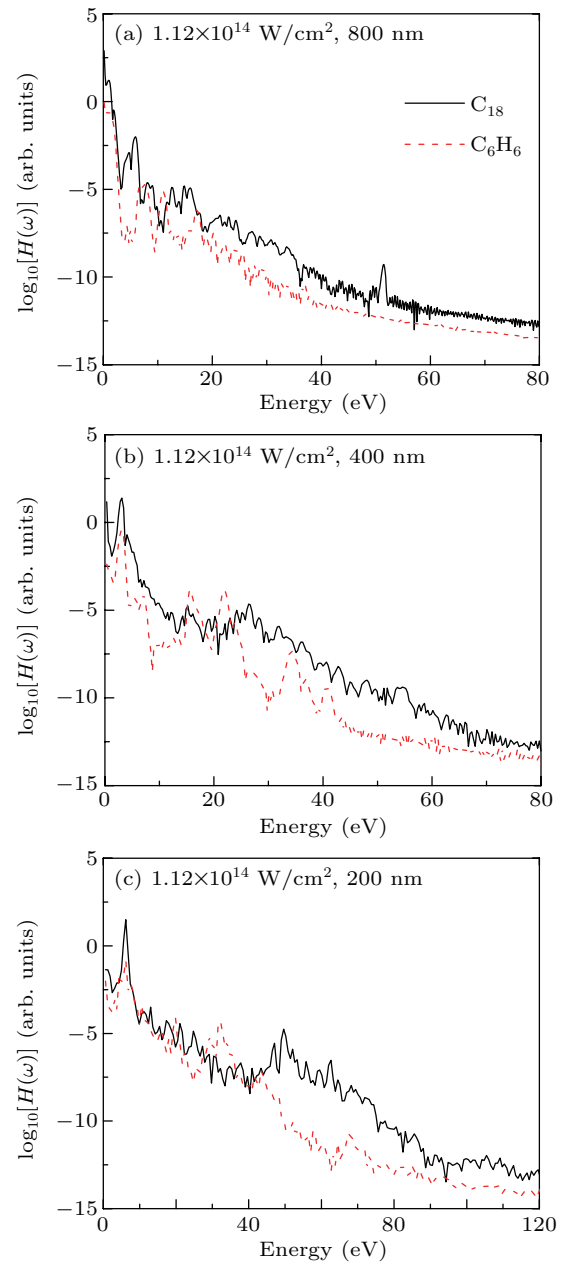


**Fig. 5.** The harmonic spectra of  $C_{18}$  and  $C_6H_6$  molecules driven by CPLP with different wavelengths: (a) 800 nm, (b) 400 nm, and (c) 200 nm.

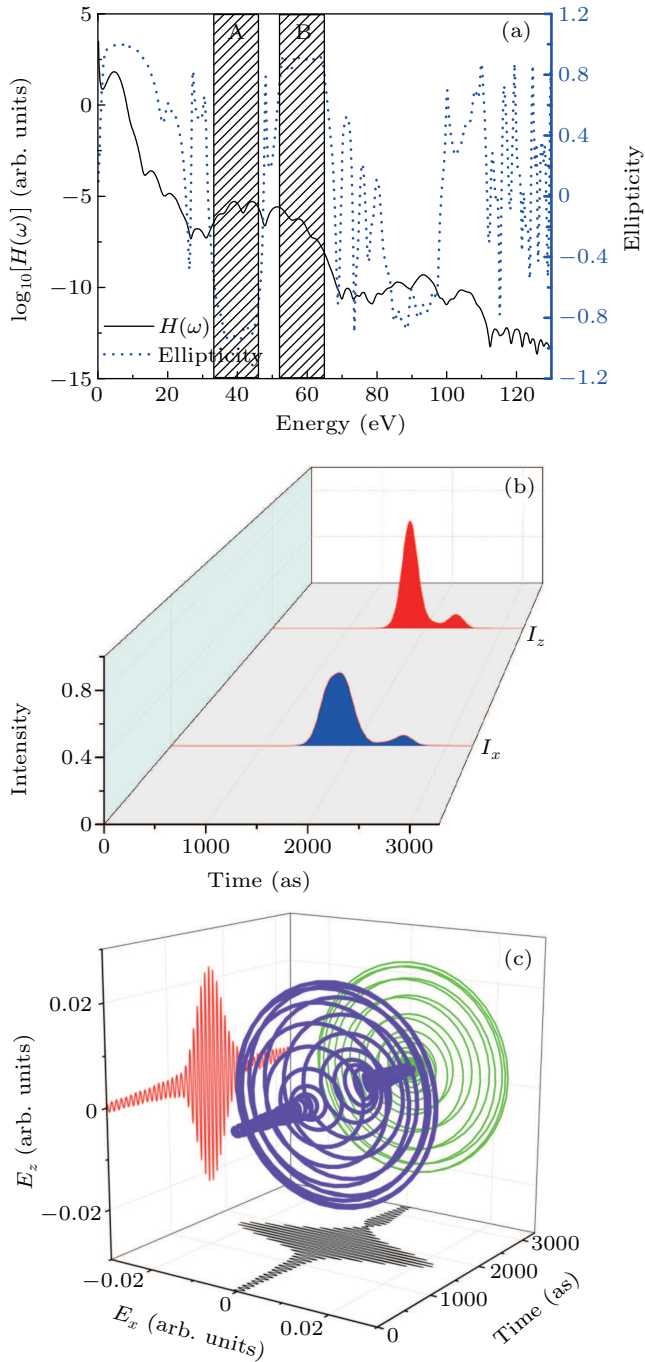


**Fig. 6.** The optimized harmonic spectrum with laser intensity  $I = 2.48 \times 10^{14} \text{ W/cm}^2$ ,  $\lambda = 200 \text{ nm}$ ,  $\tau = 1.32 \text{ fs}$ . (b) Temporal profiles of attosecond pulse,  $I_x$  (blue) and  $I_z$  (red) are field components, the unit is arbitrary. (c) The near-circularly polarized isolated attosecond pulse synthesized by harmonics (in part B) of  $\text{C}_{18}$  molecule in CPLP.

According to the sufficient analysis made above, it is found that  $\text{C}_{18}$  molecule driven by CPLP has strong harmonic emission at 200 nm. In this work, we adjust some parameters of the driving laser, such as the intensity and full width at half maximum to obtain wide harmonic plateau to synthesize IAP. The harmonic spectrum optimized with proper parameters of  $\lambda = 200 \text{ nm}$ ,  $I = 2.48 \times 10^{14} \text{ W/cm}^2$ ,  $\tau = 1.32 \text{ fs}$  is shown in Fig. 6(a), the black solid line represents the intensities of harmonics from  $\text{C}_{18}$  molecule, the blue dotted line represents the ellipticities of the total harmonics calculated. It can

be seen from the figure that there are two plateaus distributed supercontinuously in the harmonic. According to the values of ellipticity, the first plateau area is divided into two parts, the lower harmonic orders with ellipticity closing to  $-1$  are in part A (the first shaded part in Fig. 6(a)), and most higher harmonic orders with ellipticity closing to  $+1$  are in part B (the second shaded part in Fig. 6(a)), both parts have the obvious characteristics, namely, they are close to circular polarization approximately. After filtering out the harmonics ranged from 52.7 eV to 65.1 eV, the single attosecond pulse is synthesized and shown in Fig. 6(b), in which the blue part is the intensity  $I_x$  and the red parts are field components  $I_z$ , the full width at half maximum of this pulse is 250 as. The time evolution of the attosecond pulse is shown in Fig. 6(c), in which the synthesized pulse exhibits a good circular polarization character, it is confirmed that the HHG generated from  $\text{C}_{18}$  molecule driven by CPLP provides a reliable way of producing IAP.

#### 4. Conclusion

In summary, we use TDDFT to simulate the harmonic emission of the ring molecule  $\text{C}_{18}$  in a CPLP, the results are compared with the harmonic emission of  $\text{C}_6\text{H}_6$  molecule in the same laser field. The comparisons show that it is more favorable for the ionized electrons of  $\text{C}_{18}$  molecule to recombine with ions to produce intense harmonic emission under the driving of laser field, because the spatial scale of ring structure of  $\text{C}_{18}$  molecule is larger. The effects of CPLP on the harmonic emission of  $\text{C}_{18}$  molecule are discussed, with increase of the laser intensity or decrease of the wavelength, the ionized electrons are distributed around the molecule more evenly and tightly, both the probabilities of re-collision and transition increase, which lead to an increase of harmonic emission efficiency and energy cutoff. With the high intensity harmonics generated, the circularly polarized isolated attosecond pulses of opposite polarizations are obtained simultaneously after filtering. It is indicated that two attosecond pulses with opposite polarizations can be obtained simultaneously with the approach adopted in this work, and more important applications of harmonics generated are expected.

#### Acknowledgments

Project supported by the National Key Research and Development Program of China (Grant No. 2019YFA0307700) and the National Natural Science Foundation of China (Grant Nos. 12204214, 12074145, and 11627807).

#### References

- [1] Protopapas M, Keitel C H and Knight P L 1997 *Rep. Prog. Phys.* **60** 389
- [2] Yuan H Y, Yang Y J, Guo F M, Wang J and Cui Z W 2022 *Opt. Express* **30** 19745
- [3] l'Huillier A, Lompre L A, Mainfray G and Manus C 1983 *Phys. Rev. A* **27** 2503

- [4] Wu D, Guo F M, Chen J G, Wang J and Yang Y J 2020 *J. Phys. B: At. Mol. Opt. Phys.* **53** 235601
- [5] Vozzi C, Negro M, Calegari F, Sansone G, Nisoli M, De Silvestri S and Stagira S 2011 *Nat. Phys.* **7** 822
- [6] Henkel J, Witting T, Fabris D, Lein M, Knight P L, Tisch J W G and Marangos J P 2013 *Phys. Rev. A* **87** 043818
- [7] Zhao Y T, Jiang S C, Zhao X, Chen J G and Yang Y J 2020 *Opt. Lett.* **45** 2874
- [8] Zhou S S, Lan W D, Chen J G, Wang J, Guo F M and Yang Y J 2022 *Phys. Rev. A* **106** 023510
- [9] Qiao Y, Huo Y Q, Jiang S C, Yang Y J and Chen J G 2022 *Opt. Express* **30** 9971
- [10] Ayuso D, Jiménez-Galán A, Morales F, Ivanov M and Smirnova O 2017 *New J. Phys.* **19** 073007
- [11] Zhou X, Lock R, Wagner N, Li W, Kapteyn H C and Murnane M M 2009 *Phys. Rev. Lett.* **102** 073902
- [12] Graves C E *et al.* 2013 *Nat. Mater.* **12** 293
- [13] Cireasa R, Boguslavskiy A E, Pons B, Wong M C H, Descamps D, Petit S, Ruf H, Thiré N, Ferré A, Suarez J, Higuete J, Schmidt B E, Alharbi A F, Légrat F, Blanchet V, Fabre B, Patchkovskii S, Smirnova O, Mairesse Y and Bhardwaj V R 2015 *Nat. Phys.* **11** 654
- [14] Corkum P B 1993 *Phys. Rev. Lett.* **71** 1994
- [15] Fleischer A, Kfir O, Diskin T, Sidorenko P and Cohen O 2014 *Nat. Photon.* **8** 543
- [16] Fan T, Grychtol P, Knut R, Hernández-García C, Hickstein D D, Zusin D, Gentry C, Dollar F J, Mancuso C A, Hogle C W, Kfir O, Legut D, Carva K, Ellis J L, Dorney K M, Chen C, Shpyrko O G, Fullerton E E, Cohen O, Oppeneer P M, Miloevi D B, Becker A, Jaro-Becker A A, Popmintchev T, Murnane M M and Kapteyn H C 2015 *Proc. Natl. Acad. Sci. USA* **112** 14206
- [17] Chen C, Tao Z, Hernández-García C, Matyba P, Carr A, Knut R, Kfir O, Zusin D, Gentry C, Grychtol P, Cohen O, Plaja L, Becker A, Jaron-Becker A, Kapteyn H and Murnane M M 2016 *Sci. Adv.* **2** e1501333
- [18] Dixit G, Jiménez-Galán A, Medauskas L and Ivanov M 2018 *Phys. Rev. A* **98** 053402
- [19] Harada Y, Haraguchi E, Kaneshima K and Sekikawa T 2018 *Phys. Rev. A* **98** 021401
- [20] Odak S and Miloevi D B 2006 *Phys. Lett. A* **355** 368
- [21] Yuan K J and Bandrauk A D 2012 *J. Phys. B: At. Mol. Opt. Phys.* **45** 074001
- [22] Yuan K J and Bandrauk A D 2013 *Phys. Rev. Lett.* **110** 023003
- [23] Chen F, Luo J and Luo F 2015 *Opt. Commun.* **342** 68
- [24] Medauskas L, Wragg J, Hart H and Ivanov M Y 2015 *Phys. Rev. Lett.* **115** 153001
- [25] Li L, Wang Z, Li F and Long H 2017 *Opt. Quant. Electron* **49** 73
- [26] Dorney K M, Ellis J L, Hernández-García C, Hickstein D D, Mancuso C A, Brooks N, Fan T, Fan G, Zusin D, Gentry C, Grychtol P, Kapteyn H C and Murnane M M 2017 *Phys. Rev. Lett.* **119** 063201
- [27] Neufeld O and Cohen O 2018 *Phys. Rev. Lett.* **120** 133206
- [28] Zhu M F, Wang G L, Zhao S F, Li X Y and Zhou X X 2019 *J. Mod. Opt.* **66** 1467
- [29] Rego L, Román J S, Plaja L and Hernández-García C 2020 *Opt. Lett.* **45** 5636
- [30] Wardlow A and Dundas D 2016 *Phys. Rev. A* **93** 023428
- [31] Worner H J, Bertrand J B, Hockett P, Corkum P B and Villeneuve D M 2010 *Phys. Rev. Lett.* **104** 233904
- [32] Rupenyan A, Kraus P M, Schneider J and Wörner H J 2013 *Phys. Rev. A* **87** 031401
- [33] Penka E F, Couture-Bienvenue E and Bandrauk A D 2014 *Phys. Rev. A* **89** 023414
- [34] Zhu X S, Liu X, Li Y, Qin M Y, Zhang Q B, Lan P F and Lu P X 2015 *Phys. Rev. A* **91** 043418
- [35] Bandrauk A D and Yuan K J 2018 *J. Phys. B: At. Mol. Opt. Phys.* **51** 074001
- [36] Houzet J, Hertz E, Billard F, Lavorel B and Faucher O 2013 *Phys. Rev. A* **88** 023859
- [37] Skantzakis E, Chatziathanasiou S, Carpeggiani P A, Sansone S, Nayak A, Gray D, Tzallas P, Charalambidis D, Hertz E and Faucher O 2016 *Scientific Reports* **6** 39295
- [38] Sørngård S A, Simonsen S I and Hansen J P 2013 *Phys. Rev. A* **87** 053803
- [39] Chen Z Y and Qin R 2019 *Opt. Express* **27** 3761
- [40] Klemke N, Tancogne-Dejean N, Rossi G M, Yang Y, Scheiba F, Mainz R E, Sciacca G D, Rubio A, Krtner F X and Mücke O D 2019 *Nat. Commun.* **10** 1
- [41] Luu T T and Wörner H J 2021 *Eur. Phys. J. Spec. Top.* **230** 4057
- [42] Averbukh V, Alon O E and Moiseyev N 2001 *Phys. Rev. A* **64** 033411
- [43] Baer R, Neuhauser D, Dánská P R and Moiseyev N 2003 *Phys. Rev. A* **68** 043406
- [44] Žd'ánská P, Averbukh V and Moiseyev N 2003 *J. Chem. Phys.* **118** 8726
- [45] Zhou S S, Li Q Y, Guo F M, Wang J, Chen J G and Yang Y J 2021 *Chem. Phys.* **545** 111147
- [46] Kaiser K, Scriven L M, Schulz F, Gawel P, Gross L and Anderson H L 2019 *Science* **365** 1299
- [47] Runge E and Gross E K U 1984 *Phys. Rev. Lett.* **52** 997
- [48] Tancogne-Dejean N, Mücke O D, Krtner F X and Rubio A 2017 *Phys. Rev. Lett.* **118** 087403
- [49] Zhou S S, Guo J, Chen J G and Yang Y J 2017 *J. At. Mol. Sci.* **8** 18
- [50] Monfared M, Irani E and Sadighi-Bonabi R 2018 *J. Chem. Phys.* **148** 234303
- [51] Zhou S S, Yang Y J, Guo F M, Chen J G and Wang J 2020 *IEEE J. Quant. Electron.* **56** 1
- [52] Wardlow A and Dundas D 2016 *Phys. Rev. A* **93** 023428
- [53] Tancogne-Dejean N, Mücke O D, Krtner F X and Rubio A 2017 *Nat. Commun.* **8** 745
- [54] Perdew J P, Burke K and Ernzerhof M 1996 *Phys. Rev. Lett.* **77** 3865
- [55] Troullier N and Martins J L 1991 *Phys. Rev. B* **43** 1993
- [56] Kleinman L and Bylander D M 1982 *Phys. Rev. Lett.* **48** 1425
- [57] Castro A, Marques M A and Rubio A 2004 *J. Chem. Phys.* **121** 3425
- [58] De Giovannini U, Larsen A H and Rubio A 2015 *Eur. Phys. J. B* **88** 56
- [59] Alberto C, Angel R and Eberhard U K G 2015 *Eur. Phys. J. B* **88** 191
- [60] Miloevi D B, Becker W and Kopold R 2000 *Phys. Rev. A* **61** 063403
- [61] Marques M A L, Castro A, Bertsch G F and Rubio A 2003 *Phys. Commun.* **151** 60
- [62] Castro A, Appel H, Oliveira M, Rozzi C A, Andrade X, Lorenzen F, Marques M A L, Gross E K U and Rubio A 2006 *Phys. Status Solidi B* **243** 2465
- [63] Andrade X, Strubbe D, Giovannini U D, Larsen A H, Oliveira M J, Alberdi-Rodríguez J, Varas A, Theophilou I, Helbig N, Verstraete M J, Stella L, Nogueira F, Aspuru-Guzik A, Castro A, Marques M A and Rubio A 2015 *Phys. Chem. Chem. Phys.* **17** 31371
- [64] Arulmozhiraja S and Ohno T 2008 *J. Chem. Phys.* **128** 114301